Tungsten isotopes and the origin of the Moon

Thomas S. Kruijer[1,2,*] and Thorsten Kleine[1]

[1]Institut für Planetologie, University of Münster, Wilhelm-Klemm-Strasse 10, 48149 Münster, Germany.

[2]Nuclear and Chemical Sciences Division, Lawrence Livermore National Laboratory. 7000 East Avenue, Livermore, CA 94550, USA

Revised manuscript prepared for submission to *Earth and Planetary Science Letters*

Version: 12 July 2017

Main text: 6498 words

Abstract: 318 words

2 tables

6 figures

2 Supplementary tables

3 Supplementary figures

*Corresponding author:

E-mail: kruijer1@llnl.gov

Phone: +1-925-42-29262

ABSTRACT

The giant impact model of lunar origin predicts that the Moon mainly consists of impactor material. As a result, the Moon is expected to be isotopically distinct from the Earth, but it is not. To account for this unexpected isotopic similarity of the Earth and Moon, several solutions have been proposed, including (i) post-giant impact Earth–Moon equilibration, (ii) alternative models that make the Moon predominantly out of proto-Earth mantle, and (iii) formation of the Earth and Moon from an isotopically homogeneous disk reservoir. Here we use W isotope systematics of lunar samples to distinguish between these scenarios. We report high-precision ^{182}W data for several low-Ti and high-Ti mare basalts, as well as for Mg-suite sample 77215, and lunar meteorite Kalahari 009, which complement data previously obtained for KREEP-rich samples. In addition, we utilize high-precision Hf isotope and Ta/W ratio measurements to empirically quantify the superimposed effects of secondary neutron capture on measured ^{182}W compositions. Our results demonstrate that there are no resolvable radiogenic ^{182}W variations within the Moon, implying that the Moon differentiated later than 70 Ma after Solar System formation. In addition, we find that samples derived from different lunar sources have indistinguishable ^{182}W excesses, confirming that the Moon is characterized by a small, uniform ~+26 parts-per-million excess in ^{182}W over the present-day bulk silicate Earth. This ^{182}W excess is most likely caused by disproportional late accretion to the Earth and Moon, and after considering this effect, the pre-late veneer bulk silicate Earth and the Moon have indistinguishable ^{182}W compositions. Mixing calculations demonstrate that this Earth–Moon ^{182}W similarity is an unlikely outcome of the giant impact, which regardless of the amount of impactor material incorporated into the Moon should have generated a significant ^{182}W excess in the Moon. Consequently, our results imply that post-giant impact processes might have modified ^{182}W, leading to the similar ^{182}W compositions of the pre-late veneer Earth's mantle and the Moon.

Keywords: Hf-W, Moon, giant impact, magma ocean differentiation, late accretion

1. Introduction

The Moon is generally thought to have formed from debris produced during a giant impact between the proto-Earth and a roughly Mars-sized body (Cameron and Benz, 1991; Canup and Asphaug, 2001; Hartmann and Davis, 1975), but important details about this model remain incompletely understood. Recent work has focused on reconciling observed isotopic similarities between the Earth and the Moon (Armytage et al., 2012; Wiechert et al., 2001; Young et al., 2016; Zhang et al., 2012) with the prediction that in the canonical giant impact model the Moon predominantly consists of impactor material (Canup and Asphaug, 2001). Consequently, in this model the Moon is expected to show an isotopic difference relative to the Earth (Pahlevan and Stevenson, 2007), in marked contrast with the observed isotopic similarity. To explain this paradox, a variety of solutions have been proposed, including (*i*) giant impact models in which the Moon predominantly derives from the proto-Earth (Canup, 2012; Ćuk and Stewart, 2012; Reufer et al., 2012), (*ii*) post-giant impact isotopic equilibration (Pahlevan and Stevenson, 2007), and (*iii*) derivation of proto-Earth and impactor from the same isotopically homogeneous reservoir in the inner solar system (Dauphas et al., 2014; Mastrobuono-Battisti et al., 2015; Wiechert et al., 2001).

The short-lived ^{182}Hf-^{182}W system ($t_{1/2}$ = 8.9 Ma) is particularly useful to examine these issues and constrain models of lunar origin. This is because the Moon-forming impact involved mixing between impactor and proto-Earth components with presumably different ^{182}W compositions. These radiogenic ^{182}W variations result from Hf/W fractionation during core formation, which for the impactor and proto-Earth likely occurred at different times and under different conditions, ultimately leading to distinct ^{182}W compositions of proto-Earth's mantle and the impactor's mantle and core (*e.g.*, Kleine et al., 2009). Mixing of these three components during the giant impact, therefore, likely induced a ^{182}W difference between the Moon and the immediate post-giant impact mantle of the Earth. This also holds true if the Moon predominantly consists of proto-Earth mantle material, because the pre- and post-giant impact ^{182}W compositions of Earth's mantle were likely different (Kruijer et al., 2015).

Determining the ^{182}W composition of the Moon has proven difficult, because most lunar samples show cosmogenic ^{182}W excesses from neutron capture on Ta during prolonged exposure of the lunar samples to galactic cosmic rays (Leya et al., 2000). One way to overcome this problem is to analyse lunar metals, which are devoid of Ta-derived cosmogenic ^{182}W and hence should define the pre-exposure ^{182}W compositions directly (Kleine et al., 2005; Touboul et al., 2015, 2007). Using this approach, Touboul et al. (2007) neither found statistically meaningful ^{182}W differences among different lunar rock types nor between these samples and the present-day bulk silicate Earth (BSE). Nevertheless, two more recent studies, using higher precision measurement techniques, demonstrated that the Moon has a ^{182}W excess of ~25 ppm over the present-day BSE (Kruijer et al., 2015; Touboul et al., 2015). These two studies exclusively investigated KREEP-rich samples, raising the question of whether other lunar reservoirs—such as the mare basalt sources—exhibit similar or larger ^{182}W excesses. Addressing this question is important not only for precisely determining the ^{182}W composition of the bulk Moon, but also for obtaining insights into the timescale of lunar magma ocean crystallisation. This is because magma ocean crystallisation is thought to have produced compositionally distinct lunar mantle sources, including the high-Ti mare basalt sources, which are characterized by the highest Hf/W known on the Moon (*e.g.*, Righter and Shearer, 2003) Thus, if magma ocean crystallisation occurred during the lifetime of ^{182}Hf, then high-Ti mare basalts should have a radiogenic ^{182}W excess relative to other lunar rocks.

Determining the ^{182}W signatures of mare basalts is challenging because due to their high Ta/W, neutron capture effects may be significant even for weakly irradiated samples. Prior studies analyzed metal samples (Kleine et al., 2005; Touboul et al., 2007), but given the low abundance of metals in mare basalts, large sample masses must be processed to obtain sufficient W for precise isotope analyses. In this study, we therefore use a different approach and combine ^{182}W measurements on lunar whole-rock samples with high-precision Hf isotope and Ta/W ratio measurements to empirically quantify the effects of secondary neutron capture on measured ^{182}W compositions. Using this approach, we derive pre-exposure ^{182}W for different lunar source lithologies, which makes it possible (*i*) to assess the magnitude of any potential radiogenic ^{182}W variations within the Moon, and (*ii*) to

109 precisely define the ^{182}W composition of the bulk silicate Moon. We then use these results to assess
110 the timescale of lunar mantle differentiation and use the ^{182}W composition of the Moon to test current
111 giant impact models.

112 **2. Samples and analytical methods**

113 A total of 10 lunar samples were selected for combined W and Hf isotopic, as well as Ta/W
114 analyses, including 2 low-Ti mare basalts (12004, 15495), 6 high-Ti mare basalts (10057, 70017,
115 70035, 70215, 74255, 75035), Mg-suite norite 77215, and lunar meteorite Kalahari 009. The latter
116 sample was selected because of its very low cosmic ray exposure age of only ~230 yr (Nishiizumi et
117 al., 2005), and accordingly, the expectation that neutron capture effects are minimal for this sample.
118 Moreover, to permit a direct comparison to the results previously obtained for KREEP, we also
119 measured the Ta/W and Hf isotope compositions of the KREEP-rich samples investigated by Kruijer
120 et al. (2015).

121 All samples were received as rock fragments and were ultrasonically cleaned and rinsed with
122 ethanol, and then crushed and ground to a fine powder in an agate mortar. The analytical techniques
123 for sample digestion, chemical separation of W, and W isotope ratio measurements by MC-ICPMS
124 are largely based on previously developed procedures (Kruijer et al., 2015, 2014). In brief, the lunar
125 samples (~0.5-1 g) were digested in ~20-40 ml HF–HNO_3 (2:1) at 130-150 °C on a hotplate for 2-3
126 days. Then ~2-5% aliquots (equivalent to ~2 ng W and 10-20 ng Ta) were taken for the determination
127 of Ta and W concentrations by isotope dilution. For the isotope composition measurements, W was
128 separated from the sample matrix using a two-stage anion exchange chromatography (Kruijer et al.,
129 2015, 2014). While the first column separates W from most matrix elements, the second anion
130 exchange chromatography step quantitatively separates W from other high field strength elements
131 (HFSE; Ti, Zr, Hf, Ta). The Hf in these HFSE cuts was subsequently separated using Ln-spec resin as
132 described in Bast et al. (2015). Note that this chromatography step was repeated twice to ensure that
133 the final Hf cuts had Ti/Hf <0.01 and Zr/Hf <2. The total yields of the chemical separation were ~80-
134 95% for W and 50-90% for Hf. Total procedural blanks for the isotope composition analyses were

~50-100 pg W and ~20-40 pg Hf, and insignificant given the amounts analyzed (~30 ng W, ~100-1000 ng Hf).

The W and Hf isotope measurements were performed using a ThermoScientific® Neptune *Plus* MC-ICPMS in the Institut für Planetologie at the University of Münster. The procedures for high-precision W isotope analyses are described in detail elsewhere (Kruijer et al., 2015, 2014). Samples and standards for W and Hf isotope analyses were introduced using self-aspirating Cetac® C-flow or ESI® PFA nebulizers (50-60 µL/min) connected to a Cetac® Aridus II desolvator. The W isotope measurements were performed using Jet sampler and X-skimmer cones which resulted in total ion beams of ~1.5-2.5 $\times 10^{-10}$ A obtained for a ~30 ppb W standard solution at uptake rates of ~50-60 µl/min. Electronic baselines were obtained prior to each sample measurement by deflecting the beam using the electrostatic analyzer for 60 s and then subtracted from sample signal intensities. A single W isotope measurement comprised 200 cycles of 4.2 s integration time each, and each sample was measured once or twice depending on the amount of W available for analysis. Small isobaric interferences from ^{184}Os and ^{186}Os on W isotope ratios were corrected by monitoring interference-free ^{188}Os, and were smaller than 10 parts-per-million (ppm) on $^{182}W/^{184}W$ and hence insignificant. Instrumental mass bias was corrected by internal normalization to $^{186}W/^{184}W = 0.92767$ (denoted '6/4') using the exponential law. Note that we only used $^{186}W/^{184}W$-normalized data to avoid normalizations involving ^{183}W; the latter can be biased by a small analytical artefact on ^{183}W introduced during sample preparation, as observed in this and several earlier studies (*e.g.*, Cook and Schönbächler, 2016; Kruijer et al., 2012; Willbold et al., 2011). The Hf isotope analyses were performed using standard sampler and 'H' skimmer cones and all major 'non-radiogenic' Hf isotopes (^{177}Hf, ^{178}Hf, ^{179}Hf, ^{180}Hf) were measured simultaneously. Total ion beams of ~3.5-4.5 $\times 10^{-10}$ were obtained for a ~150 ppb Hf standard solution at uptake rates of ~50 µl/min. Electronic baselines were obtained prior to each sample measurement by deflecting the beam using the electrostatic analyzer for 60 s and then subtracted from sample signal intensities. A single Hf isotope measurement comprised 200 cycles of 4.2 s integration time each but sample solutions were measured 4-6 times to improve the precision. Potential isobaric interferences from ^{180}W and ^{180}Ta on ^{180}Hf were corrected by monitoring

interference-free ^{183}W and ^{181}Ta, and were negligible (<10 ppm on $^{180}Hf/^{177}Hf$). Instrumental mass bias was corrected by internal normalization to $^{179}Hf/^{177}Hf = 0.7325$ using the exponential law. The W and Hf isotope analyses of samples were bracketed by measurements of terrestrial solution standards (prepared from Alfa Aesar metal for W and from AMES metal for Hf) and results are reported as μ-unit (*i.e.*, parts-per-million) deviations from the mean values of the bracketing solution standards. The accuracy and reproducibility of the methods were assessed through analyses of terrestrial rock standards (BCR-2, BHVO-2) that were digested, processed and analyzed alongside the lunar samples. The mean $\mu^{i}W$ and $\mu^{i}Hf$ values of the analyzed rock standards are indistinguishable from the solution standard measurements, demonstrating that the analyses are accurate (Tables S1 and S2).

To determine W and Ta concentrations of the lunar samples by isotope dilution, aliquots were spiked with a mixed ^{180}Hf-^{180}Ta-^{183}W tracer (Weyer et al., 2002). The chemical separation of Hf, Ta, and W by anion exchange chromatography followed previously established methods (Kleine et al., 2004; Weyer et al., 2002). Total procedural blanks for the isotope dilution measurements were ~17 pg W, ~1 pg Ta, and ~6 pg Hf, and were insignificant for all samples. All isotope dilution measurements were performed on the Neptune *Plus* MC-ICPMS at Münster, and for Hf and W followed the procedures described in Kruijer et al. (2014). For the Ta isotope measurements, instrumental mass bias was corrected relative to Ta solution standards measured before and after each sample by normalization to $^{180}Ta/^{181}Ta = 0.0001198$ (Weyer et al., 2002) using the exponential law. Potential Hf interferences on mass 180 were corrected by monitoring ^{178}Hf, and interference corrections on $^{180}Ta/^{181}Ta$ were smaller than 2% for most samples. Some of the lunar samples investigated here were previously analyzed for Ta concentrations, also using isotope dilution (Münker et al. 2003, Münker, 2010). For these samples the Ta concentrations determined in the two studies agree to within ~10% (Fig. S1). Following Weyer et al. (2002) we therefore adopted an uncertainty of ~5% (2σ) for the Ta concentration measurements.

3. Results

All investigated lunar samples exhibit $\mu^{182}W$ values that are distinctly higher than the terrestrial value (Table 1). Both the low-Ti and high-Ti mare basalts show variably elevated $\mu^{182}W$, from ~+50 ppm to ~+750 ppm, consistent with previous work (Kleine et al., 2005; Touboul et al., 2007). The same mare basalt samples show strongly variable Hf isotope compositions (Table S1, Fig. S2), resulting in correlated variations of $\mu^{178}Hf$ (up to +230 ppm) and $\mu^{180}Hf$ (down to –380 ppm). In contrast, lunar meteorite Kalahari 009 shows no resolvable Hf isotope anomaly, and a $\mu^{182}W$ of +25±11 ppm (2 s.d.), *i.e.*, very similar to the value previously determined for KREEP (Kruijer et al., 2015; Touboul et al., 2015). Furthermore, Mg-suite norite 77215 shows an only slightly higher $\mu^{182}W$ (+35±10 ppm) and a small Hf isotope anomaly (Table 1). The KREEP-rich samples studied here also display variable $\mu^{182}W$ and Hf isotope compositions (Kruijer et al., 2015). For several of these samples, we re-measured the Hf isotope compositions to higher precision (Table S1). The values thus obtained are in excellent agreement with those of previously obtained, but generally more precise. The Ta/W of the investigated lunar samples show large variations (Table 1), with high-Ti mare basalts (Ta/W ~4.5-25) having distinctly higher and more variable Ta/W than the low-Ti mare basalts (~3.6-5.5) and KREEP (~1.9-2.5).

4. Homogeneous ^{182}W within the Moon

4.1. Pre-exposure ^{182}W compositions of lunar samples

The lunar samples investigated in the present study show coupled $\mu^{178}Hf$ and $\mu^{180}Hf$ variations that are consistent with the effects of secondary neutron capture (Table S1, Fig. S2). As Hf isotopes capture neutrons at similar (mostly epithermal) energies as W, these Hf isotope variations can be used as an empirical neutron dosimeter to quantify cosmogenic ^{182}W effects (*e.g.*, Kruijer et al., 2015). The production of cosmogenic ^{182}W in lunar whole-rock samples occurs through the reaction $^{181}Ta(n,\gamma)^{182}Ta(\beta^-)^{182}W$ (Leya et al., 2000), and thus not only depends on the neutron dose that a lunar sample received (as quantified using Hf isotopes), but also on its Ta/W. Consequently, lunar samples with a common pre-exposure $\mu^{182}W$ (*i.e.*, unaffected by neutron capture) but variable neutron capture

212 effects should exhibit positive linear correlations between measured $\mu^{182}W$ and $\mu^{180}Hf \times (Ta/W)$ or
213 $\mu^{178}Hf \times (Ta/W)$. The lunar samples analyzed in this study define such correlations (Fig. 1, 2, S3),
214 indicating that the ^{182}W variations observed for samples derived from a common mantle reservoir
215 (*e.g.*, high-Ti mare basalts) are cosmogenic in origin. The pre-exposure $\mu^{182}W$ values obtained from
216 these correlations are indistinguishable from each other, regardless of whether $\mu^{180}Hf$ or $\mu^{178}Hf$ are
217 used as neutron dosimeters. Nevertheless, because the $\mu^{180}Hf$ data provide more precise pre-exposure
218 $\mu^{182}W$ values, and for consistency with earlier studies (Kruijer et al., 2015; Sprung et al., 2013), we
219 used $\mu^{180}Hf \times (Ta/W)$ to quantify neutron capture effects on $\mu^{182}W$.

220

221 *4.1.1. Non-KREEP samples*

222 The high-Ti mare basalts analyzed here exhibit a well-defined, neutron capture–induced $\mu^{182}W$
223 *vs.* $\mu^{180}Hf \times (Ta/W)$ correlation (Fig. 1a). Of note, another, more strongly irradiated high-Ti mare
224 basalt (79155), whose $\mu^{182}W$, $\mu^{180}Hf$ and Ta/W had previously been determined (Kleine et al., 2005;
225 Sprung et al., 2013), plots on the extension of this correlation line. Together, the high-Ti mare basalts
226 are characterized by a common pre-exposure $\mu^{182}W$ of +15±15 ppm (95% conf.) as defined by the
227 intercept obtained by linear regression. This pre-exposure $\mu^{182}W$ is indistinguishable from but more
228 precise than the mean $\mu^{182}W$ of 11±28 ppm (95% conf., $n = 5$) previously obtained for metal separates
229 from five high-Ti mare basalts (Touboul et al., 2007).

230 The two low-Ti mare basalts investigated here (12004, 15495) plot on the same $\mu^{182}W$ *vs.*
231 $\mu^{180}Hf \times (Ta/W)$ correlation as the high-Ti mare basalts (Fig. 1b). Linear regression of the low-Ti
232 mare basalt data yields a pre-exposure $\mu^{182}W$ of +28±13 ppm (95% conf., $n = 2$), indistinguishable
233 from that of the high-Ti mare basalts. A regression of all mare basalts together results in a common
234 pre-exposure $\mu^{182}W$ of +23±10 ppm (95% conf., $n = 8$), which again is consistent with the value of
235 +12±13 ppm (95% conf., $n = 9$) previously reported by Touboul et al. (2007). However, in contrast to
236 this previous study we find that mare basalts exhibit a resolved common ~23 ppm $\mu^{182}W$ excess over
237 the present-day BSE.

Lunar meteorite Kalahari 009 shows a small $\mu^{182}W$ excess of +25±11 (2s.d.) and no resolvable Hf isotope anomaly (Table 1), indicating that neutron capture effects are minimal in this sample. This is consistent with the very low cosmic ray exposure age (~230 yr) of this sample (Nishiizumi et al., 2005). Consequently, the measured $\mu^{182}W$ = +25±11 does not require any correction for neutron capture, and defines the pre-exposure $\mu^{182}W$ value of Kalahari 009 directly. In contrast, Mg-suite norite 77215 shows a slightly larger $\mu^{182}W$ excess of +37±10, but also a small Hf isotope anomaly indicative of neutron capture effects. The measured $\mu^{182}W$ of 77215 can be corrected for neutron capture effects using the slope of the $\mu^{182}W$ vs. $\mu^{180}Hf \times (Ta/W)$ correlation obtained from the mare basalts (Fig. 1c). This results in a pre-exposure $\mu^{182}W$ of +31±11 for 77215, which is indistinguishable from the values obtained for the mare basalts and Kalahari 009. The similarity in pre-exposure $\mu^{182}W$ among these rocks is consistent with the observation that all samples combined plot on a single $\mu^{182}W$ vs. $\mu^{180}Hf \times (Ta/W)$ correlation line (Fig. 1c), which yields a precisely defined pre-exposure $\mu^{182}W$ for these samples of +26±6 ppm (95% conf., n = 10).

4.1.2. KREEP-rich samples

The KREEP-rich samples analyzed by Kruijer et al. (2015) all plot on a single $\mu^{182}W$ *vs.* $\mu^{180}Hf$ correlation, implying that these samples should have very similar Ta/W. To validate that this is the case, we measured the Ta and W concentrations on digestion aliquots of these samples. These analyses show that the KREEP-rich samples indeed exhibit a very narrow range in Ta/W (~1.90 to ~2.56; Table 1). Moreover, as some of the Hf isotope data reported in Kruijer et al. (2015) were determined on different digestions than those analyzed for W isotopes, we also re-measured the Hf isotope compositions of these samples using the very same digestion aliquots as analyzed for W (Fig. 2a). Collectively, the combined $\mu^{182}W$, $\mu^{180}Hf$, and Ta/W data for KREEP-rich samples yield well-defined correlations and pre-exposure values, both in $\mu^{182}W$ *vs.* $\mu^{180}Hf$ space (+27±3 ppm; Fig. 2a) and in $\mu^{182}W$ *vs.* $\mu^{180}Hf \times (Ta/W)$ space (+26±3 ppm; Fig. 2b). These values are also consistent with previously reported values of +27±4 ppm from Kruijer et al. (2015), as well as +21±5 ppm from Touboul et al. (2015).

Finally, one curious observation is that the slopes of the $\mu^{182}W$ *vs.* $\mu^{180}Hf \times (Ta/W)$ correlation lines are different for KREEP (–27±1) and mare basalts (−35±1). The exact cause of this difference in slopes remains unclear, but one possibility is that it reflects different neutron energy spectra which vary because of the distinct target chemistry of KREEP-rich versus mare basalt samples (*e.g.*, Sprung et al., 2013 and references therein).

4.2. Implications for the timescale of lunar magma ocean differentiation

The distinct lunar mantle reservoirs produced during magma ocean crystallisation have variable Hf/W ratios, where the source of high-Ti mare basalts is thought to be characterized by distinctly higher Hf/W of ~40-80 compared to Hf/W ~10–20 for KREEP (*e.g.*, Fonseca et al., 2014; Kleine et al., 2005; Münker, 2010; Righter and Shearer, 2003; Touboul et al., 2007). Thus, if magma ocean crystallisation occurred within the lifetime of ^{182}Hf, then these reservoirs should have evolved to distinct $\mu^{182}W$ values. However, our results demonstrate that low-Ti and high-Ti mare basalts as well as KREEP have indistinguishable $\mu^{182}W$ (Fig. 3). Moreover, both Mg-suite norite 77215 and meteorite Kalahari 009 also have pre-exposure $\mu^{182}W$ values that are indistinguishable from those of the mare basalts and KREEP. While constraining the source Hf/W of Kalahari 009 and Mg-suite norite 77215 is not straightforward, the radiogenic initial $^{176}Hf/^{177}Hf$ isotopic composition and old age of ~4.2 Ga of Kalahari 009 (Sokol et al., 2008) indicate that the mantle source of this sample had undergone strong incompatible element depletion early in lunar history. As such, the mantle source of Kalahari 009 would likely have had a high Hf/W, but again the $\mu^{182}W$ of Kalahari 009 is indistinguishable from that of KREEP, which is characterized by the lowest Hf/W of the distinct sources produced during crystallisation of the lunar magma ocean.

Taken together, the homogeneous $\mu^{182}W$ of the investigated lunar sample suite, despite the large range of source Hf/W ratios, indicates that lunar differentiation occurred after the effective life-time of ^{182}Hf. As such, these data can be used to estimate the earliest possible time of lunar differentiation, defined here as the time of isolation of the high-Hf/W source reservoir of the high-Ti

mare basalts. Within the error limits of the ^{182}W data, the highest possible $\mu^{182}W$ of the high-Ti mare basalt source is +33 ppm (based on the combined pre-exposure $\mu^{182}W$ of +23+10 ppm for the mare basalts, Fig. 1b), whereas the lowest possible $\mu^{182}W$ of KREEP is +23 ppm ($\mu^{182}W$ = +26+3 ppm, Fig. 2b). Thus, any possible ^{182}W excess in the high-Ti mare basalts must be smaller than ~10 ppm. The Hf/W ratio of the high-Ti mare basalts has been estimated to be between ~40 and ~80, whereas that of KREEP probably is between ~10 and ~20 (Righter and Shearer, 2003). Using these Hf/W ratios and the $\mu^{182}W$ excess of <10 ppm from above shows that the high-Ti mare basalt source must have been established later than ~70 Ma after solar system formation, *i.e.* later than ~4.5 Ga (Fig. 4). This time constraint is consistent with the 4.35-4.37 Ga ages obtained for the major period of lunar differentiation using several independent methods. More specifically, both the (most reliable) Sm-Nd isochron ages for lunar crustal rocks, the Sm-Nd and Lu-Hf model ages of KREEP, and the average Sm-Nd model age of the mare basalt sources, as well as a peak in Pb-Pb ages observed in lunar zircons all appear to converge at 4.35-4.37 Ga (see summary in Borg et al., 2015 and references therein). Collectively, these relatively young ages, combined with the lack of ^{182}W heterogeneity in the Moon, support the idea that the major period of differentiation on the Moon occurred relatively late.

More recently, Barboni et al. (2017) argued, based on Hf isotopic data for lunar zircons, that the major differentiation of the Moon occurred earlier, at 4.51±0.01 Ga. This inferred age only marginally overlaps with the maximum age of lunar differentiation inferred above from the ^{182}W data for high-Ti mare basalts. In particular, the ^{182}W data would be consistent with differentiation of the Moon at 4.51 Ga only for the smallest difference in source Hf/W ratios *and* the largest possible difference in $\mu^{182}W$ (Fig. 4). Thus, although these two age estimates overlap within their uncertainties, it is in fact unlikely that they are consistent with each other. The exact reason for this discrepancy remains unclear, and resolving this issue will require a better understanding of the significance of the old inferred ages for individual lunar zircon grains versus the model ages inferred for large geochemical reservoirs on the Moon.

4.3. Origin of ^{182}W excess in the Moon

The results of the present study demonstrate that the different lunar rock types all exhibit indistinguishable pre-exposure $\mu^{182}W$, and that they are all characterized by an ^{182}W excess over the present-day BSE (Fig. 3). Of note, the investigated lunar samples derive from different landing sites and mantle sources, and in some cases (lunar meteorite Kalahari 009) likely also from different locations on the Moon than the Apollo samples. As such, we interpret the weighted mean $\mu^{182}W$ of +26±3 ppm (95% conf., n=5; Fig. 3) obtained for these samples to be representative for the bulk silicate Moon. In a prior study, Touboul et al. (2007) also found uniform ^{182}W compositions for KREEP and mare basalts, but that study did not find a resolvable ^{182}W difference between the Moon and the present-day BSE. This may either reflect unaccounted neutron capture burn-out effects on W isotopes in the lunar metals analyzed by Touboul et al. (2007) or more likely the poorer analytical resolution achievable when the Touboul et al. (2007) study was conducted. Either way, the new pre-exposure $\mu^{182}W$ values obtained here demonstrate that the Moon is characterized by a well-resolved ^{182}W excess over the present-day BSE.

The $\mu^{182}W$ difference of +26 ppm observed between the Moon and the present-day BSE may in principal have three different origins. One possibility is that the ^{182}W excess reflects a radiogenic ^{182}W difference between the Moon and the Earth. This would require different Hf/W ratios of the BSE and Moon and formation of the Moon within the lifetime of ^{182}Hf. However, most studies have argued that the Moon formed after extinction of ^{182}Hf (*e.g.*, Touboul et al., 2007; Halliday, 2008; Borg et al., 2011; Jacobson et al., 2014; Bottke et al. 2015). Moreover, the Hf/W ratio of both the Moon and the BSE have rather large uncertainties (*e.g.*, Kleine and Walker, 2017), and so it is also unclear if these ratios are sufficiently different to produce a significant ^{182}W excess in the Moon. A second option is that the lunar ^{182}W excess originated during the giant impact and reflects a larger fraction of impactor material within the Moon. We will show in Section 5 below that such an ^{182}W excess is in fact expected in the giant impact model of lunar origin. A corollary of this is that any ^{182}W *difference* between the Moon and the BSE cannot be used to firmly establish the age of the Moon, even if their Hf/W ratios were sufficiently different. This is because for the Moon it is not possible to distinguish

between a radiogenic ^{182}W anomaly and a ^{182}W anomaly that arises from mixing of proto-Earth and impactor material during the giant impact. In other words, it is unclear as to whether the Earth's mantle and the Moon *initially* had identical ^{182}W compositions, but this requirement must be fulfilled for any chronological interpretation of the ^{182}W data.

The third possibility to account for the ^{182}W difference between the present-day BSE and the Moon is late accretion. Late accretion is commonly defined as the addition of on average broadly chondritic material (the 'late veneer') to the mantles of the Earth and Moon following the formation of the Moon. As the late veneer is enriched in W (typically ~150–200 ppb W) and characterized by a low $\mu^{182}W$ of about –190 ppm, late accretion leads to an overall decrease of the $\mu^{182}W$ composition of the mantle (*e.g.*, Willbold et al., 2011). However, the estimated proportion of late-accreted materials added to the silicate Earth (~0.5 to 0.8 wt.%) and the Moon (~0.02 wt.%) are very different (Day and Walker, 2015), suggesting that late accretion predominantly affected the ^{182}W composition of Earth's mantle and not that of the Moon (Kruijer et al., 2015; Touboul et al., 2015). For instance, whereas late accretion probably lowered the $\mu^{182}W$ of the BSE by ~15–30 ppm, the $\mu^{182}W$ value of the Moon remained essentially unchanged. Thus, unless the amount of late-accreted material added to the Moon is more than an order of magnitude higher than estimated based on the highly siderophile element systematics of lunar rocks (*e.g.*, Day and Walker, 2015), late accretion inevitably resulted in a ^{182}W difference between the Moon and the silicate Earth. Of note, the $\mu^{182}W$ excess of ~+26 ppm of the Moon over the present-day BSE is fully consistent with the effects expected from disproportional late accretion to the Earth and Moon (Kruijer et al., 2015; Touboul et al., 2015). In detail, the magnitude of this effect on $\mu^{182}W$ depends on the mass and composition assumed for the late veneer as well as on the W concentration of the BSE. As such the calculated pre-late veneer $\mu^{182}W$ of the BSE may have been between ~+10 and ~+50 ppm (Kleine and Walker, 2017). Thus, although the ~26 ppm ^{182}W excess of the Moon may not only be due to late accretion, no *resolvable* $\mu^{182}W$ difference between the pre-late veneer BSE and the Moon remains once the effects of late accretion are taken into account. As a result, there is currently neither solid evidence for a ^{182}W signature from the impactor in the Moon nor for the existence of a radiogenic ^{182}W difference between the Earth and the Moon. In

summary, considering the uncertainties on the calculated $\mu^{182}W$ composition of the pre-late veneer BSE shows that the $\mu^{182}W$ compositions for the pre-late veneer BSE and the Moon are indistinguishable and that any *possible* ^{182}W excess in the Moon prior to late accretion likely is smaller than ~15 ppm.

5. Implications for the origin of the Moon

The $\mu^{182}W$ similarity between the pre-late veneer BSE and the Moon is generally consistent with the isotopic similarity observed for other elements, such as Ti, Si, and O (Armytage et al., 2012; Herwartz et al., 2014; Wiechert et al., 2001; Young et al., 2016; Zhang et al., 2012). However, whereas the isotopic similarity for the latter elements can potentially be accounted for by accretion of the Earth and impactor from an isotopically homogeneous inner disk reservoir (Dauphas et al., 2014; Mastrobuono-Battisti et al., 2015) or by making the Moon predominantly out of the Earth's mantle (Canup, 2012; Ćuk and Stewart, 2012; Reufer et al., 2012), such mechanisms are not easily reconciled with the similarity in $\mu^{182}W$. This is because variations in $\mu^{182}W$ are not nucleosynthetic in origin (unlike for instance for Ti), but instead are due to radiogenic ingrowth of ^{182}W in the proto-Earth and impactor mantles following metal-silicate separation in these bodies. In this light, the Moon should be considered a three-component mixture consisting of proto-Earth's mantle, impactor mantle, and impactor core (the proto-Earth's core is typically not considered to have taken part in the formation of the Moon; *e.g.*, Canup, 2004). As these three components are likely characterized by different $\mu^{182}W$ and because they are mixed in different proportions during the giant impact, producing similar $\mu^{182}W$ in the Moon and Earth's mantle seems quite unlikely (Kruijer et al., 2015). However, Dauphas et al. (2014) used an inversion method to calculate, for given giant impact scenarios, the Hf/W and $\mu^{182}W$ of the impactor mantle necessary to obtain the observed ^{182}W signature of the Moon. The Hf/W and $\mu^{182}W$ values predicted by these model calculations are reasonable in the sense that they provide model timescales for core formation in the impactor of between 10-20 Ma after CAI formation, as expected for the differentiation of a Mars-sized body. On this basis, Dauphas et al. (2014) concluded that the similar ^{182}W compositions of Earth's mantle and the Moon are consistent with current giant

impact models of lunar origin. Wade and Wood (2016) took a different approach and assumed that the Moon predominantly derived from Earth's mantle. These authors argued that in this case the ^{182}W data are best explained by an impact of a Mars-sized, strongly reduced impactor onto an oxidized proto-Earth, combined with only limited equilibration of the impactor core with Earth's mantle.

While these prior studies demonstrate that the ^{182}W compositions of the Moon and Earth's mantle can be produced in a giant impact, they both have to resort to happenstance to account for the indistinguishable ^{182}W compositions of the pre-late veneer BSE and the Moon. Here we, therefore, take a different approach and aim to assess the likelihood of producing the similar ^{182}W compositions of the pre-late veneer BSE and the Moon during the giant impact. To this end, we calculated the *expected* ^{182}W composition of the Moon resulting from mixing of proto-Earth mantle material with variable proportions of impactor mantle and core (see online Supplementary Material). The ^{182}W composition of the Moon calculated in this manner depends on several parameters, including the impactor composition, the mass fraction of impactor material (both mantle and core) in the Moon, the impactor-to-Earth ratio, the degree to which the impactor core equilibrated with Earth's mantle, and the metal-silicate partition coefficient for W during post-giant impact core formation in the Earth and during core formation in the Moon (Table 2). The calculations were performed separately using fixed mass fractions of 0, 0.2 and 0.8 for the amount of impactor material in the Moon. In the last two cases the mass fraction of impactor core material was varied randomly between 0 and 0.025; an impactor core fraction of 0.025 was taken as the upper bound because the mass fraction of the lunar core is estimated to be <2.5 % (*e.g.*, Rai and van Westrenen, 2014; Righter, 2002; Weber et al., 2011). The impactor-to-Earth ratio was assumed to be 0.04 and 0.15 to cover the range of impactor sizes proposed in recent models (*e.g.*, Ćuk and Stewart, 2012; Wade and Wood, 2016). Note that the model of Canup (2012) involves a much larger impactor with an impactor-to-Earth ratio of ~0.5, but incorporating this into the model does not change the outcome of the calculations. The ^{182}W composition of impactor mantle and core depend on the metal-silicate partition coefficients (D_W) and on the timing of core formation in the impactor. We assumed D_W values between 5 and 100, corresponding to an oxidized versus reduced impactor, and core formation ages between 5 and 20 Ma

after CAI formation. This timescale for core formation is reasonable for a Mars-sized impactor (*e.g.*, Dauphas and Pourmand, 2011; Mezger et al., 2013). The degree of equilibration of the impactor core with proto-Earth's mantle (k) was considered a free parameter and was randomly varied between no ($k = 0$) and full equilibration ($k = 1$). Finally, D_W for core formation in the Earth following the giant impact was varied between 20 and 100 [*i.e.*, the range of values typically considered for Earth; (Cottrell et al., 2009; Wade and Wood, 2005)], and D_W during lunar core formation was varied between 1 and 100. This large range of values reflects the uncertainty regarding the conditions of lunar core formation and the dependency of D_W on the S content of the lunar core. For instance, Wade and Wood (2016) argued that the lunar core might be S-rich, in which case W would have behaved essentially lithophile. Except for the mass fraction of impactor material in the Moon, all these parameters have been varied randomly within the given bounds (Table 2).

Figure 5 summarizes the results of the modeling for three different mass fractions of impactor material in the Moon. In all three cases the observed composition of the Moon plots within the field of the calculated expected compositions for the Moon. This is consistent with results of a prior study, showing that for a variety of impact scenarios it is possible to match the observed ^{182}W composition of the Moon with reasonable Hf-W isotopic systematics of the impactor (Dauphas et al., 2014). However, the results of our calculations also show that the observed composition of the Moon does not plot near the center of the field of expected ^{182}W compositions, but rather at the edge of these fields. This is especially true for cases in which the Moon predominantly consists of impactor material and illustrates that producing the Earth-Moon ^{182}W similarity is an unlikely outcome of the giant impact (Fig. 5). Our calculations show that the probability of producing similar ^{182}W compositions of the pre-late veneer Earth's mantle and the Moon to within 15 ppm is <5% for models in which the Moon consists of less than 20% impactor material, and <1% for cases in which the Moon consists for more than 80% impactor material (Fig. 6). While these calculations show that the probability for producing any given ^{182}W composition of the Moon is small (*i.e.*, there is not one specific composition that is predominantly produced), they also show that by far the most likely outcome of the giant impact is a significant ^{182}W excess in the Moon. For instance, a ^{182}W anomaly of >+50 ppm

451 is calculated for more than ~70% of the cases, and a ^{182}W anomaly of >+100 ppm is calculated for
452 more than ~50% of the cases.

453 Our calculations demonstrate that the indistinguishable ^{182}W compositions of the pre-late
454 veneer Earth's mantle and the Moon are an unexpected outcome of the giant impact, regardless of
455 how much impactor material was incorporated into the Moon. Instead, the giant impact should have
456 led to a significant ^{182}W excess for the Moon. As such the ^{182}W data suggest strongly that post-giant
457 impact processes modified the ^{182}W composition of the Moon, such as for instance post-giant impact
458 equilibration between the Earth and Moon. Although it has been shown that O isotope equilibration
459 may be possible by means of a shared silicate atmosphere of a terrestrial magma ocean and the proto-
460 lunar magma disk (Pahlevan and Stevenson, 2007), this process would be less effective for refractory
461 elements such as Ti and probably also W (Zhang et al., 2012). Nevertheless, recently a new type of
462 giant impact model was proposed, in which the Moon formed through a high-energy, high-angular-
463 momentum giant impact (Ćuk et al. 2016; Lock et al., 2016; Wang and Jacobsen, 2016). This model
464 predicts that the Earth's mantle and atmosphere together with the proto-lunar accretion disk form a
465 well-mixed reservoir from which the Moon ultimately condenses. As in this model the Earth and
466 Moon would derive from the same homogenized reservoir, they would have acquired identical
467 isotopic compositions (except for possible mass-dependent isotope fractionations).

468 Another possibility for post-giant impact modifications of the Moon's ^{182}W composition is the
469 addition of significant mass to the Moon after the Moon-forming giant impact. As noted above, highly
470 siderophile element systematics suggest that the amount of late-accreted material added to the Moon
471 was very low. However, addition of a large differentiated projectile, coupled with metal-silicate
472 equilibration and segregation of metal into the lunar core would not be visible in the highly
473 siderophile element systematics. This is because all the highly siderophile elements added by the
474 projectile, together with those that had already accumulated in the lunar mantle during previous late-
475 accretionary events, would have been transferred to the lunar core. By contrast, the equilibration of
476 the projectile's core with the lunar mantle would have led to a significant decrease of the μ^{182}W of the
477 lunar mantle. Of note, it was recently suggested that the Procellarum basin might have formed by a

large impact on the lunar near side and it was also shown that this event would have added sufficient mass to lower the $\mu^{182}W$ composition of the lunar mantle (or more accurately, the area of the Moon from which most if not all samples derive) by ~100 ppm (Zhu et al., 2017). Thus, prior to this putative event, the Moon would have had a significant ^{182}W excess, as predicted by our mixing calculations (Fig. 5, 6). In this model, the good agreement between the lunar $\mu^{182}W$ of ~26 ppm and the expected effects for disproportional late accretion to the Earth and Moon would be somewhat coincidental, however.

6. Conclusions

Our results demonstrate that there are no radiogenic ^{182}W variations within the Moon, indicating that lunar differentiation occurred later than 70 Ma after CAI formation. Moreover, the uniform ^{182}W excess found for different lunar rock types confirms that the Moon is characterized by a ^{182}W excess over the present-day BSE. This excess most likely reflects disproportional late accretion to the Earth and Moon. Once the effects of late accretion have been taken into account, the ^{182}W compositions of the pre-late veneer BSE and the Moon are indistinguishable to within 15 ppm. Mixing calculations indicate that this ^{182}W similarity is an unlikely outcome of the giant impact, which should have resulted in a significant ^{182}W difference between the Earth and the Moon. Consequently, our results seem to require post-giant impact processes affecting ^{182}W, such as a high-energy, high-angular momentum giant impact onto the Earth or secondary large impacts onto the Moon, adding sufficient mass to modify ^{182}W.

Acknowledgements:

We thank Alan Brandon and an anonymous reviewer for their constructive and helpful reviews, and Fred Moynier for his editorial efforts. We gratefully acknowledge Ryan Zeigler, CAPTEM and NASA for providing the Apollo lunar samples for this study. We are thankful to E. Scherer for providing a split of the HFSE spike, and to A. Bischoff for providing a sample of Kalahari 009.

Finally, we thank B.E.J. Kruijer for his assistance. This study was performed under the auspices of the US DOE by Lawrence Livermore National Laboratory under Contract DE-AC52-07NA27344 with release number LLNL-JRNL-731059. This work was funded by the Deutsche Forschungsgemeinschaft (SFB TRR 170 subproject C3-1). This is TRR 170 publication no. 13.

References

Armytage, R.M.G., Georg, R.B., Williams, H.M., Halliday, A.N., 2012. Silicon isotopes in lunar rocks: Implications for the Moon's formation and the early history of the Earth. Geochim. Cosmochim. Acta 77, 504–514. doi:10.1016/j.gca.2011.10.032

Arevalo, R., McDonough W.F. (2008) Tungsten geochemistry and implications for understanding the Earth's interior. Earth and Planetary Science Letters 272, 656-665.

Bast, R., Scherer, E.E., Sprung, P., Fischer-Gödde M., Stracke A., Mezger, K., 2015. A rapid and efficient ion-exchange chromatography for Lu–Hf, Sm–Nd, and Rb–Sr geochronology and the routine isotope analysis of sub-ng amounts of Hf by MC-ICP-MS. Journal of Analytical Atomic Spectrometry 30, 2323-2333. doi: 10.1039/C5JA00283D.

Borg, L.E., Connelly J.N., Boyet M., Carlson R.W., 2011. Chronological evidence that the Moon is either young or did not have a global magma ocean. Nature 477, 70-72.

Borg, L.E., Gaffney A.M., Shearer C.K., 2015. A review of lunar chronology revealing a preponderance of 4.34–4.37 Ga ages. Meteoritics and Planetary Science 50, 715-732.

Bottke, W.F. et al., 2015. Dating the Moon-forming impact event with asteroidal meteorites. Science 348, 321-323.

Barboni, M., Boehnke, P., Keller, B., Kohl, *I.E.*, Schoene, B., Young, E.D., McKeegan, K.D. (2017) Early formation of the Moon 4.51 billion years ago. Science Advances 3, e1602365.

Cameron, A.G.W., Benz, W., 1991. The origin of the moon and the single impact hypothesis IV. Icarus 92, 204–216. doi:10.1016/0019-1035(91)90046-V

Canup, R.M., 2012. Forming a Moon with an Earth-like composition via a giant impact. Science 338, 1052–5. doi:10.1126/science.1226073

Canup, R.M. (2004) Dynamics of lunar formation. Annual Review of Astronomy and Astrophysics 42, 441-475.

Canup, R.M., Asphaug, E., 2001. Origin of the Moon in a giant impact near the end of the Earth's formation. Nature 412, 708–12. doi:10.1038/35089010

Carlson, R.W., Borg, L.E., Gaffney, A.M., Boyet, M., 2014. Rb-Sr, Sm-Nd and Lu-Hf isotope systematics of the lunar Mg-suite: the age of the lunar crust and its relation to the time of Moon formation. Phil. Trans. R. Soc. A. 372. doi:0.1098/rsta.2013.0246

Cook, D.L., Schönbächler, M., 2016. High-precision measurement of W isotopes in Fe–Ni alloy and the effects from the nuclear field shift. J. Anal. At. Spectrom. doi:10.1039/C6JA00015K

Cottrell, E., Walter, M.J., Walker, D., 2009. Metal–silicate partitioning of tungsten at high pressure and temperature: Implications for equilibrium core formation in Earth. Earth Planet. Sci. Lett. 281, 275–287. doi:10.1016/j.epsl.2009.02.024

Ćuk, M., Stewart, S.T., 2012. Making the Moon from a fast-spinning Earth: a giant impact followed by resonant despinning. Science 338, 1047–52. doi:10.1126/science.1225542

Çuk, M, Hamilton, D.P., Stewart, S.T., 2016. Tidal evolution of the Moon from a high-obliquity, high-angular-momentum Earth. Nature 539, 402–406.

Dauphas, N., Burkhardt, C., Warren, P., Teng, F.-Z., 2014. Geochemical arguments for an Earth-like Moon-forming impactor. Philos. Trans. R. Soc. A. 372, 20130244.

Dauphas, N., Pourmand, A., 2011. Hf-W-Th evidence for rapid growth of Mars and its status as a planetary embryo. Nature 473, 489–92. doi:10.1038/nature10077

Day, J.M.D., Walker, R.J., 2015. Highly siderophile element depletion in the Moon. Earth Planet. Sci. Lett. 423, 114–124.

Fonseca, R.O.C., Mallmann, G., Sprung, P., Sommer, J.E., Heuser, A., Speelmanns, I.M., Blanchard, H., 2014. Redox controls on tungsten and uranium crystal/silicate melt partitioning and implications for the U/W and Th/W ratio of the lunar mantle. Earth Planet. Sci. Lett. 404, 1–13. doi:10.1016/j.epsl.2014.07.015

Halliday, A.N., 2008. A young Moon-forming giant impact at 70 to 110 million years accompanied by late-stage mixing, core formation and degassing of the Earth. Philosophical Transactions of the Royal Society of London, Series A 366: 4163–4181.

Hartmann, W.K., Davis, D.R., 1975. Satellite-sized planetesimals and lunar origin. Icarus 24, 504–515. doi:10.1016/0019-1035(75)90070-6

Herwartz, D., Pack, A., Friedrichs, B., Bischoff, A., 2014. Identification of the giant impactor Theia in lunar rocks. Science 344, 1146–50. doi:10.1126/science.1251117

Jacobson S.A., et al., 2014. Highly siderophile elements in Earth's mantle as a clock for the Moon-forming impact. Nature 508, 84-87.

Kleine, T., Mezger, K., Münker, C., Palme, H., Bischoff, A., 2004. 182Hf-182W isotope systematics of chondrites, eucrites, and martian meteorites: Chronology of core formation and early mantle differentiation in Vesta and Mars. Geochim. Cosmochim. Acta 68, 2935–2946. doi:10.1016/j.gca.2004.01.009

Kleine, T., Palme, H., Mezger, K., Halliday, A.N., 2005. Hf-W chronometry of lunar metals and the age and early differentiation of the Moon. Science 310, 1671–4. doi:10.1126/science.1118842

Kleine, T., Touboul, M., Bourdon, B., Nimmo, F., Mezger, K., Palme, H., Yin, Q.Z., Jacobsen, S.B., Halliday, A.N., 2009. Hf–W chronology of the accretion and early evolution of asteroids and terrestrial planets. Geochim. Cosmochim. Acta 73, 5150–5188.

Kleine, T., Walker, R.J., 2017. Tungsten isotopes in planets. Annu. Rev. Earth Planet. Sci. In press.

König, S. et al. (2011) The Earth's tungsten budget during mantle melting and crust formation. Geochimica et Cosmochimica Acta 75, 2119-2136.

Kruijer, T.S., Kleine, T., Fischer-Gödde, M., Burkhardt, C., Wieler, R., 2014. Nucleosynthetic W isotope anomalies and the Hf-W chronometry of Ca-Al-rich inclusions. Earth Planet. Sci. Lett.

403, 317–327. doi:10.1016/j.epsl.2014.07.003

Kruijer, T.S., Kleine, T., Fischer-Gödde, M., Sprung, P., 2015. Lunar tungsten isotopic evidence for the late veneer. Nature 520, 534–537. doi:10.1038/nature14360

Kruijer, T.S., Sprung, P., Kleine, T., Leya, I., Burkhardt, C., Wieler, R., 2012. Hf–W chronometry of core formation in planetesimals inferred from weakly irradiated iron meteorites. Geochim. Cosmochim. Acta 99, 287–304. doi:10.1016/j.gca.2012.09.015

Leya, I., Wieler, R., Halliday, A.N., 2000. Cosmic-ray production of tungsten isotopes in lunar samples and meteorites and its implications for Hf–W cosmochemistry. Earth Planet. Sci. Lett. 175, 1–12. doi:10.1016/S0012-821X(99)00295-2

Lock, S.J., Stewart, S.T., Petaev, M.I., Leinhardt, Z.M., Mace, M., Jacobsen, S.B., Ćuk, M., 2016. A new model for lunar origin: Equilibration with Earth beyond the hot spin stability limit, in: Lunar and Planetary Science Conference #2881.

Mastrobuono-Battisti, A., Perets, H.B., Raymond, S.N., 2015. A primordial origin for the compositional similarity between the Earth and the Moon. Nature 520, 212–215. doi:10.1038/nature14333

Mezger, K., Debaille, V., Kleine, T., 2013. Core Formation and Mantle Differentiation on Mars. Space Sci. Rev. 174, 27–48. doi:10.1007/s11214-012-9935-8

Münker C., Pfänder J. A., Weyer S., Büchl A., Kleine T. and Mezger K., 2003. Evolution of planetary cores and the Earth–Moon system from Nb/Ta systematics. Science 301, 84–87.

Münker, C., 2010. A high field strength element perspective on early lunar differentiation. Geochim. Cosmochim. Acta 74, 7340–7361. doi:10.1016/j.gca.2010.09.021

Nishiizumi, K., Welten, K.C., Bischoff, A., 2005. Kalahari 008/009 - The shortest exposure age of all meteorites., in: 68th Annual Meeting of the Meteoritical Society (#5270), Gatlinburg.

Pahlevan, K., Stevenson, D.J., 2007. Equilibration in the aftermath of the lunar-forming giant impact. Earth Planet. Sci. Lett. 262, 438–449. doi:10.1016/j.epsl.2007.07.055

Rai, N., van Westrenen, W., 2014. Lunar core formation: New constraints from metal–silicate partitioning of siderophile elements. Earth Planet. Sci. Lett. 388, 343–352. doi:10.1016/j.epsl.2013.12.001

Reufer, A., Meier, M.M.M., Benz, W., Wieler, R., 2012. A hit-and-run giant impact scenario. Icarus 221, 296–299. doi:10.1016/j.icarus.2012.07.021

Righter, K., 2002. Does the Moon have a metallic core? Constraints from giant impact modelling and siderophile elements. Icarus 158, 1–13.

Righter, K., Shearer, C.K., 2003. Magmatic fractionation of Hf and W: constraints on the timing of core formation and differentiation in the Moon and Mars. Geochim. Cosmochim. Acta 67, 2497–2507. doi:10.1016/S0016-7037(02)01349-2

Sokol, A.K., Fernandes, V.A., Schulz, T., Bischoff, A., Burgess, R., Clayton, R.N., Münker, C., Nishiizumi, K., Palme, H., Schultz, L., Weckwerth, G., Mezger, K., Horstmann, M., 2008. Geochemistry, petrology and ages of the lunar meteorites Kalahari 008 and 009: New constraints on early lunar evolution. Geochim. Cosmochim. Acta 72, 4845–4873. doi:10.1016/j.gca.2008.07.012

621 Sprung, P., Kleine, T., Scherer, E.E., 2013. Isotopic evidence for chondritic Lu/Hf and Sm/Nd of the
622 Moon. Earth Planet. Sci. Lett. 380, 77–87. doi:10.1016/j.epsl.2013.08.018

623 Touboul, M., Kleine, T., Bourdon, B., Palme, H., Wieler, R., 2007. Late formation and prolonged
624 differentiation of the Moon inferred from W isotopes in lunar metals. Nature 450, 1206–9.
625 doi:10.1038/nature06428

626 Touboul, M., Puchtel, I.S., Walker, R.J., 2015. Tungsten isotopic evidence for disproportional late
627 accretion to the Earth and Moon. Nature 520, 530–533. doi:10.1038/nature14355

628 Wade, J., Wood, B.J., 2005. Core formation and the oxidation state of the Earth. Earth Planet. Sci.
629 Lett. 236, 78–95. doi:10.1016/j.epsl.2005.05.017

630 Wade, J., Wood, B.J., 2016. The oxidation state and mass of the Moon-forming impactor, Earth and
631 Planetary Science Letters. doi:10.1016/j.epsl.2016.02.053

632 Wang, K., Jacobsen, S.B., 2016. Potassium isotopic evidence for a high-energy giant impact origin of
633 the Moon. Nature 538, 487–490.

634 Weber, R.C., Lin, P.-Y., Garnero, E.J., Williams, Q., Lognonné, P., 2011. Seismic detection of the
635 lunar core. Science 331, 309–12. doi:10.1126/science.1199375

636 Weyer, S., Mu, C., Rehka, M., 2002. Determination of ultra-low Nb , Ta , Zr and Hf concentrations
637 and the chondritic Zr / Hf and Nb / Ta ratios by isotope dilution analyses with multiple collector
638 ICP-MS. Chemical Geology 187, 295–313.

639 Wiechert, U., Halliday, A.N., Lee, D.-C., Snyder, G.A., Taylor, L.A., Rumble, D., 2001. Oxygen
640 Isotopes and the Moon-Forming Giant Impact. Science (80-.). 294, 345–348.

641 Willbold, M., Elliott, T., Moorbath, S., 2011. The tungsten isotopic composition of the Earth's mantle
642 before the terminal bombardment. Nature 477, 195–8. doi:10.1038/nature10399

643 Young, E.D., Kohl, *I.E.*, Warren, P.H., Rubie, D.C., Jacobson, S.A., Morbidelli, A., 2016. Oxygen
644 isotopic evidence for vigorous mixing during the Moon-forming giant impact. Science (80-.).
645 351.

646 Zhang, J., Dauphas, N., Davis, A.M., Leya, I., Fedkin, A., 2012. The proto-Earth as a significant
647 source of lunar material. Nat. Geosci. 5, 251–255. doi:10.1038/ngeo1429

648 Zhu, M.H., Wünnemann, K., Potter, R.W.K., Kleine, T., Morbidelli, A., 2017. Forming the Moon's
649 nearside-farside dichotomies via giant impact, in: Lunar and Planetary Science Conference
650 #1851.

651

652

Figure captions

Fig. 1: $\mu^{182}W$ *vs.* $\mu^{180}Hf \times (Ta/W)$ for non-KREEP samples. (a) High-Ti mare basalts, (b) low-Ti and high-Ti mare basalts, (c) low-Ti and high-Ti mare basalts, Mg-suite norite 77215 and Kalahari 009. Error bars denote external uncertainties (2σ, Table 1). Inset shows the data near the intercept of the regression line. Data for 79155 are from Kleine et al. (2005) and Sprung et al. (2013).

Fig. 2: (a) $\mu^{182}W$ *vs.* $\mu^{180}Hf$, and (b) $\mu^{182}W$ *vs.* $\mu^{180}Hf \times (Ta/W)$ for KREEP-rich samples. Error bars denote external uncertainties (2σ, see Table 1). Tungsten isotope data for KREEP-rich samples are from Kruijer et al. (2015).

Fig. 3: Pre-exposure $\mu^{182}W$ of different lunar source lithologies. Error bars denote external uncertainties (95% conf.) on pre-exposure $\mu^{182}W$. Hashed area shows the weighted mean $\mu^{182}W$ value and the associated 95% conf. limits. Note that the mean $\mu^{182}W$ is based on data obtained in this study and Kruijer et al. (2015), and that the KREEP value from Touboul et al. (2015) is plotted for comparison.

Fig. 4: Plot of $\mu^{182}W$ *vs.* time (in Ma) after Solar System formation. Solid curves show the expected $\mu^{182}W$ anomalies in the high-Ti mare basalt sources (with Hf/W between ~40 and ~80) relative to KREEP ($\mu^{182}W = 26\pm3$, Hf/W between ~10 and ~20) as a function of differentiation time [calculated using the Solar System initial $^{182}Hf/^{180}Hf$ of $(1.018\pm0.043)\times10^{-4}$ (Kruijer et al., 2014), and using $^{180}Hf/^{184}W = 1.18 \times Hf/W$]. The shaded orange area shows the observed, possible measured $\mu^{182}W$ excess in the high-Ti mare basalts relative to the $\mu^{182}W$ value of KREEP.

Fig. 5: Expected $\mu^{182}W$ and Hf/W of the Moon (small red dots) in three different giant impact scenarios: (a) No impactor material in the Moon (h = 0), (b) 20% impactor mantle material in the

678 Moon (h = 0.2), and (c) 80% impactor mantle material in the Moon (h = 0.8). Shown for comparison
679 is the observed composition of the Moon (round open symbol). See Section 5 for details.

680

681 **Fig. 6:** Histograms showing the predicted $\mu^{182}W$ difference between the Moon and Earth's mantle.
682 Shown are the result for three different giant impact scenarios (a-c), each involving a different mass
683 fraction of impactor mantle (h) within the Moon. The observed composition of the Moon is the
684 maximum possible observed $\mu^{182}W$ excess in the Moon as determined in this study (see Section 5 for
685 details).

686

687

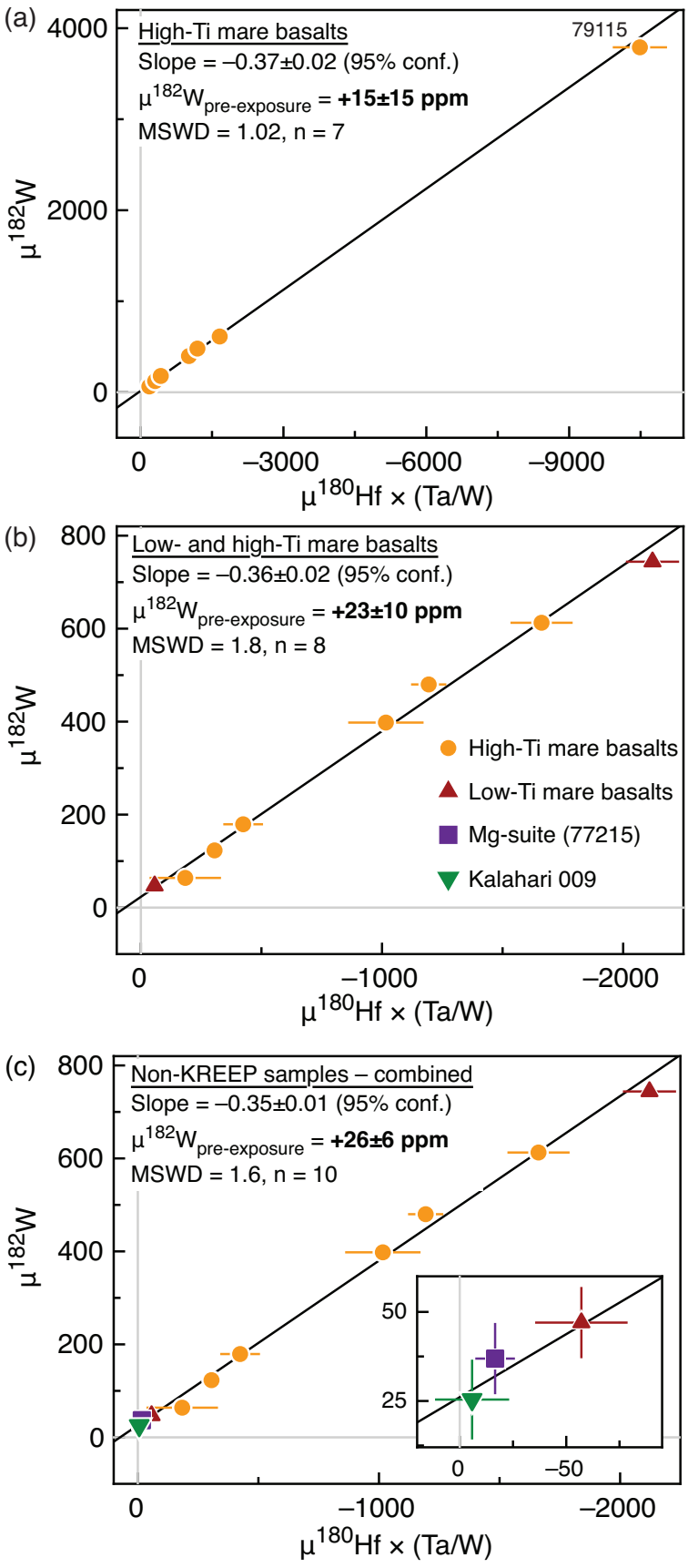
(a)
High-Ti mare basalts
Slope = –0.37±0.02 (95% conf.)
μ182Wpre-exposure = +15±15 ppm
MSWD = 1.02, n = 7
79115
μ182W
μ180Hf × (Ta/W)
(b)
Low- and high-Ti mare basalts
Slope = –0.36±0.02 (95% conf.)
μ182Wpre-exposure = +23±10 ppm
MSWD = 1.8, n = 8
High-Ti mare basalts
Low-Ti mare basalts
Mg-suite (77215)
Kalahari 009
(c)
Non-KREEP samples – combined
Slope = –0.35±0.01 (95% conf.)
μ182Wpre-exposure = +26±6 ppm
MSWD = 1.6, n = 10

Fig_1

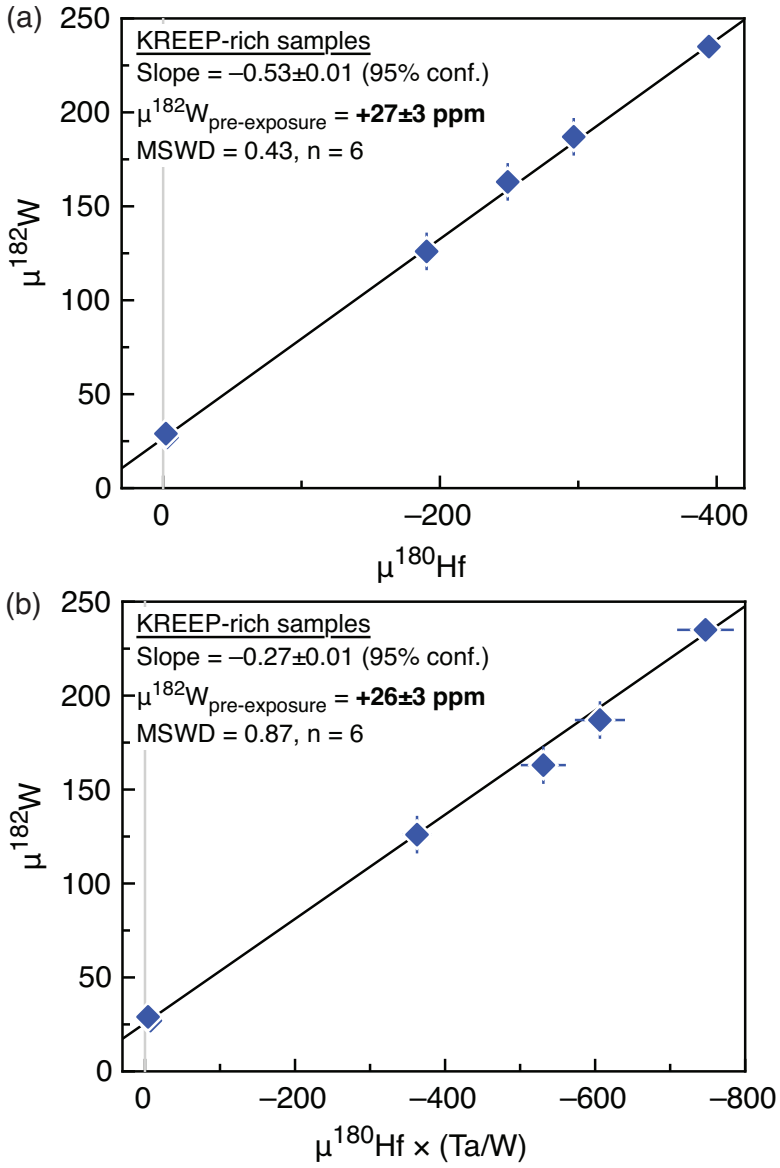
(a)
KREEP-rich samples
Slope = –0.53±0.01 (95% conf.)
μ182Wpre-exposure = +27±3 ppm
MSWD = 0.43, n = 6
μ182W
μ180Hf
(b)
KREEP-rich samples
Slope = –0.27±0.01 (95% conf.)
μ182Wpre-exposure = +26±3 ppm
MSWD = 0.87, n = 6
μ182W
μ180Hf × (Ta/W)

Fig_2

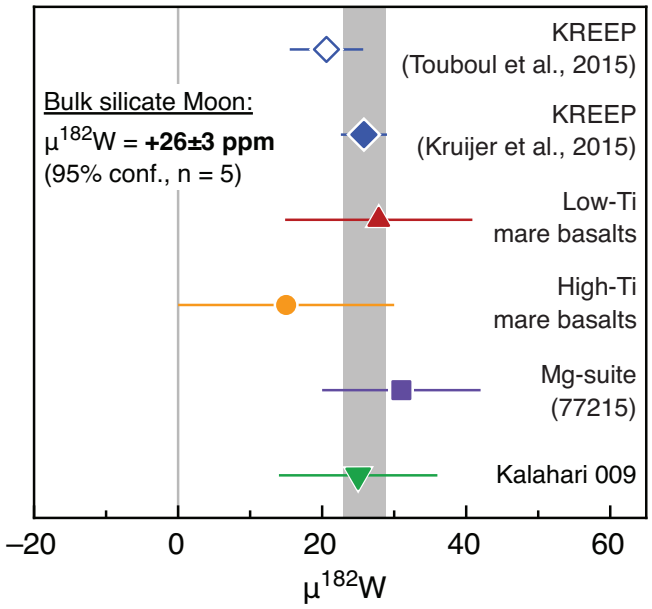
KREEP
(Touboul et al., 2015)
KREEP
(Kruijer et al., 2015)
Low-Ti
mare basalts
High-Ti
mare basalts
Mg-suite
(77215)
Kalahari 009
Bulk silicate Moon:
μ182W = +26±3 ppm
(95% conf., n = 5)
–20
0
20
40
60
μ182W

Fig_3

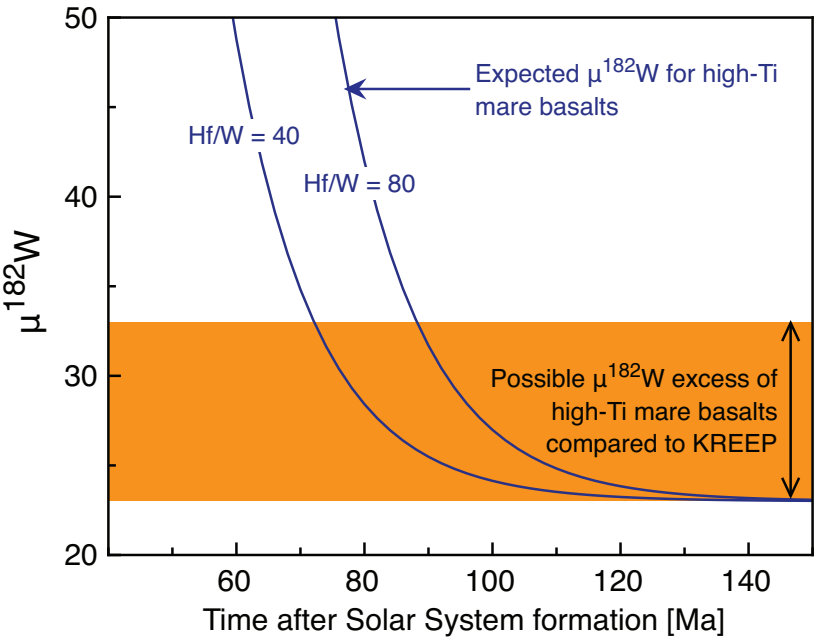
50
40
30
20
μ182W
60
80
100
120
140
Time after Solar System formation [Ma]
Hf/W = 40
Hf/W = 80
Expected μ182W for high-Ti mare basalts
Possible μ182W excess of high-Ti mare basalts compared to KREEP

Fig_4

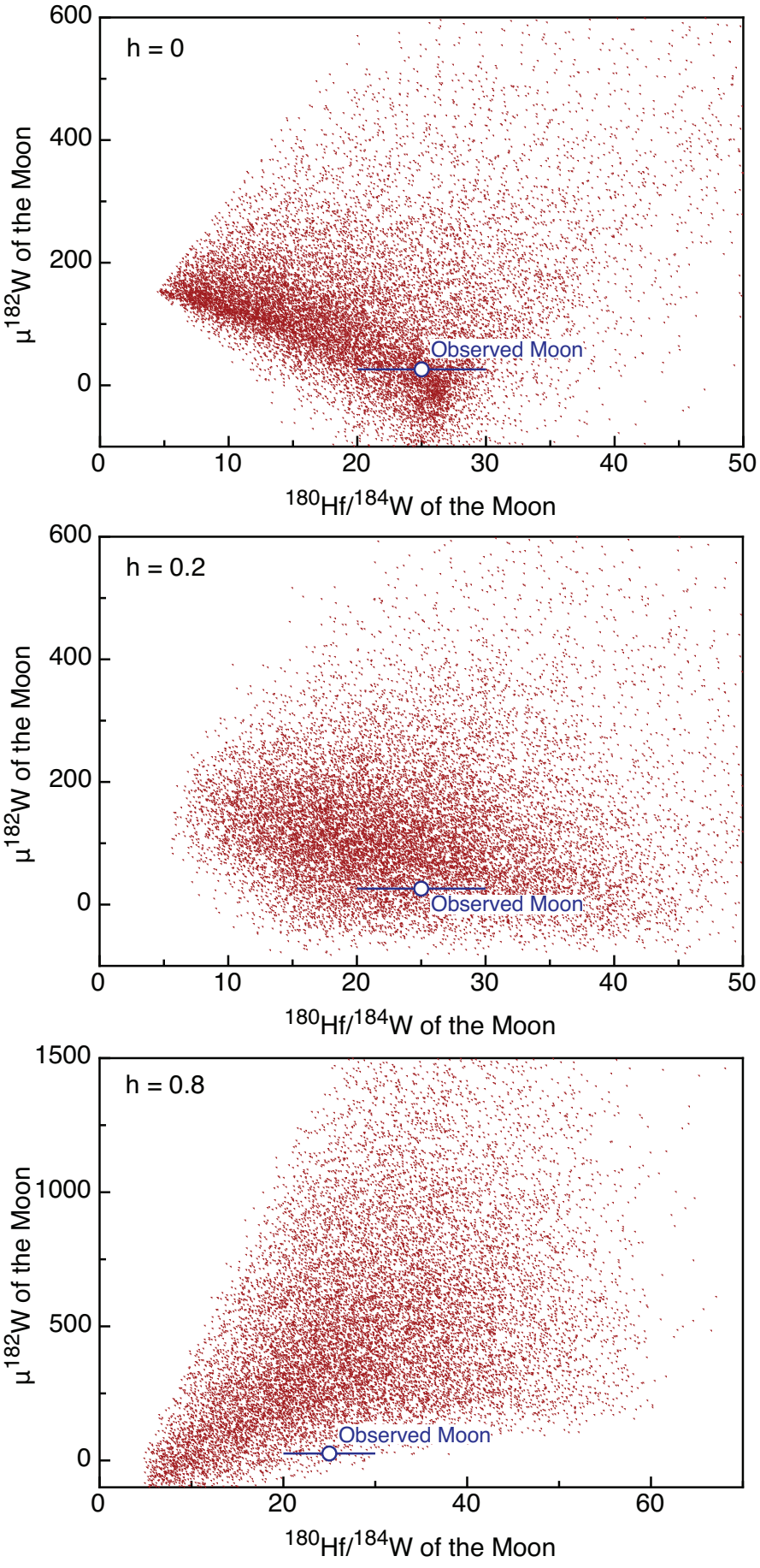
h = 0
Observed Moon
μ182W of the Moon
180Hf/184W of the Moon
h = 0.2
Observed Moon
μ182W of the Moon
180Hf/184W of the Moon
h = 0.8
Observed Moon
μ182W of the Moon
180Hf/184W of the Moon

Fig_5

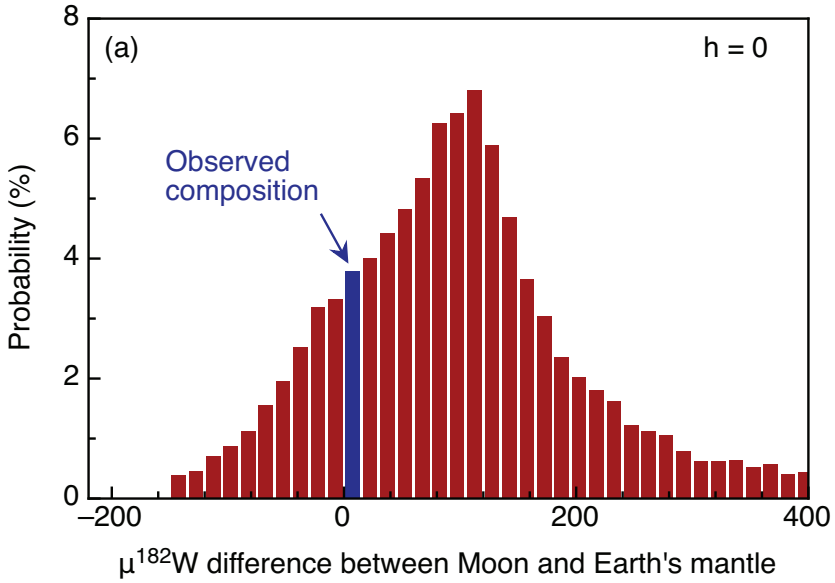
(a)
h = 0
Observed composition
Probability (%)
8
6
4
2
0
–200
0
200
400
μ182W difference between Moon and Earth's mantle

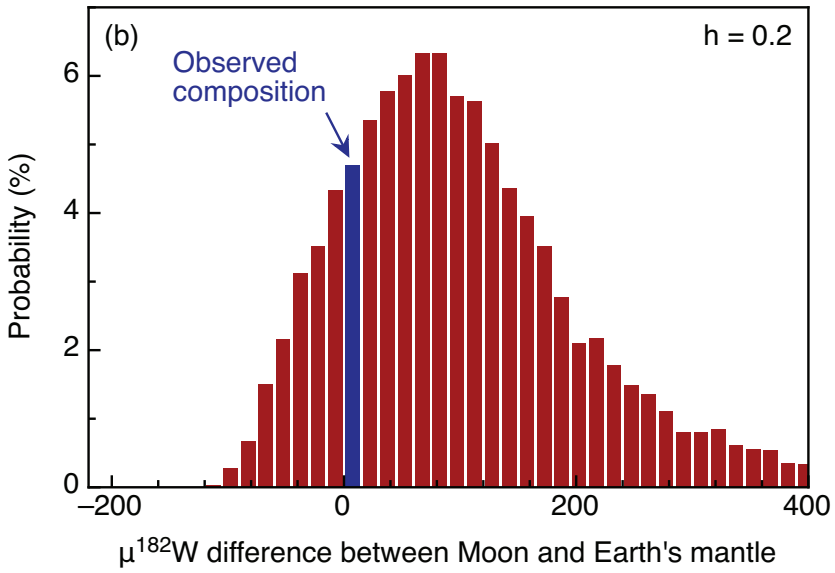
(b)
h = 0.2
Observed composition
Probability (%)
6
4
2
0
–200
0
200
400
μ182W difference between Moon and Earth's mantle

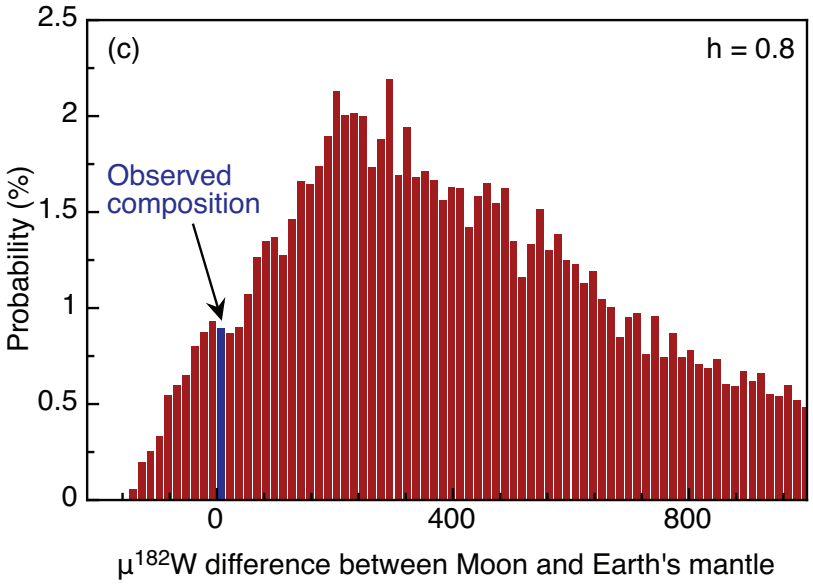
(c)
h = 0.8
Observed composition
Probability (%)
2.5
2
1.5
1
0.5
0
0
400
800
μ182W difference between Moon and Earth's mantle

Fig_6

Table 1
Tungsten and Hf isotope compositions as well as Ta, W, and Hf concentrations of lunar samples.

Sample	Specific	ID	Mass (g)	Ta (ppb)	W (ppb)	Hf (ppm)	Ta/W (molar) (2σ)		$\mu^{180}Hf$ [1] (95% conf.)		$\mu^{180}Hf \times (Ta/W)$ (95% conf.)		$\mu^{182}W_{meas.}$ [2] (2σ)	
Low-Ti mare basalts														
12004	161	BS01	0.512	385	106	3.22	3.69	± 0.19	-15	± 6	-57	± 22	47	± 10
15495	202	CI01	0.560	374	67.8	3.03	5.61	± 0.28	-378	± 5	-2122	± 110	744	± 10
High-Ti mare basalts														
10057	278	CI02	0.571	1805	401	16.6	4.57	± 0.23	-67	± 6	-306	± 32	123	± 10
70017	525	CI03	0.545	1499	63.1	8.48	24.1	± 1.2	-42	± 6	-1016	± 156	397	± 15
70035	182	CI04	0.567	2058	101	12.5	20.7	± 1.0	-58	± 2	-1194	± 73	480	± 10
70215	324	CL01	0.581	1405	58.5	6.56	24.4	± 1.2	-17	± 3	-424	± 82	179	± 12
74255	214	BS02	0.512	1409	55.8	8.55	25.6	± 1.3	-7	± 6	-184	± 148	64	± 10
75035	226	CL02	0.577	1861	86.5	11.3	21.9	± 1.1	-76	± 4	-1662	± 129	613	± 10
79155 †	160						20.3	± 1.0	-516	± 11	-10485	± 570	3790	± 100
Mg-suite norite														
77215	275	CI05	0.557	400	212	3.48	1.92	± 0.10	-9	± 5	-17	± 9	37	± 10
Lunar meteorite														
Kalahari 009		CD06-07	0.977	31.5	16.5	0.422	1.94	± 0.10	-3	± 9	-6	± 17	25	± 11
KREEP-rich samples ‡														
12034	120	BF03	0.096	2489	1328	20.6	1.90	± 0.10	-190	± 4	-363	± 19	126	± 10
14163	921	BI03	0.158	2782	1492	22.9	1.89	± 0.09	-394	± 3	-747	± 38	235	± 4
14310	676	BF02	0.102	2214	1101	19.3	2.04	± 0.10	-297	± 7	-606	± 33	187	± 10
14321	1827	BF01	0.085	884	351	7.51	2.56	± 0.13	-3	± 1	-7	± 2	27	± 4
68115	112	BG03	0.179	ND	ND	ND			-2	± 5	-4	± 10	29	± 5
62235	122	BG02	0.119	2012	959	19.6	2.13	± 0.11	-249	± 6	-531	± 30	163	± 10

[1]Internally normalized to $^{179}Hf/^{177}Hf = 0.7325$ using the exponential law. Reported uncertainties denote 95% conf. limits of the mean (Table S1).
[2]Internally normalized to $^{186}W/^{184}W = 0.92767$ using the exponential law. Reported uncertainties represent the external reproducibility as derived from terrestrial rock standards (Kruijer et al., 2015), or the standard error (2s.e.) as obtained from internal run statistics, whichever is larger.
†79155: Hf isotope data from Sprung et al. (2013) and W isotope data and Ta, W, and Hf concentrations from Kleine et al. (2005).
‡Tungsten isotope data for KREEP-rich samples from Kruijer et al. (2015).

Table 2
Model parameters used in mass-balance for calculating the ^{182}W composition of the Moon.

Parameter	Description	Value	Comments / Reference(s)
g	Mass fraction of impactor in the Earth	0.04–0.15	Variable
γ	Mass fraction of the mantle in the Earth and the impactor	0.68	Constant
k	Mass fraction of impactor core equilibrated with the Earth's mantle	0–1	Variable
h	Mass fraction of the Moon that was initially impactor mantle material	0, 0.2, or 0.8	
f	Mass fraction of the Moon that was initially impactor core material	0–0.025	Variable
$D^{\mathrm{W}}_{\mathrm{Earth}}$	Metal–silicate partition coefficient for W in Earth after the giant impact	20–100	Variable Cottrell et al. (2009) Wade and Wood (2005)
$D^{\mathrm{W}}_{\mathrm{Moon}}$	Metal–silicate partition coefficient for W in Moon	1–100	Variable Cottrell et al. (2009) Wade & Wood (2016)
$D^{\mathrm{W}}_{\mathrm{Impactor}}$	Metal–silicate partition coefficient for W in impactor	5–100	Variable Cottrell et al. (2009)
t	Time of core formation in impactor after CAI formation	5–20 Ma	Variable
$(\mathrm{Hf/W})_{\mathrm{chondrites}}$	Hf/W of chondrites	1.14	Kleine et al. (2009)
$(\mathrm{Hf/W})_{\mathrm{BSE}}$	Hf/W of the bulk silicate Earth (BSE)	~23	Arevalo & McDonough (2008) Kleine et al. (2009) König et al. (2011)
$(\mu^{182}\mathrm{W})_{\mathrm{chondrites}}$	Present-day μ^{182}W composition of chondrites	–190±10	Kleine et al. (2009)
$(\mu^{182}\mathrm{W})_{\mathrm{CAI}}$	Initial μ^{182}W composition of CAIs	–349±7	Kruijer et al. (2014)
$(^{182}\mathrm{Hf}/^{180}\mathrm{Hf})_{\mathrm{CAI}}$	Initial ^{182}Hf/^{180}Hf of CAIs	$(1.018\pm0.043)\pm10^{-4}$	Kruijer et al. (2014)